nature biotechnology

Inhibition of natural antisense transcripts *in vivo* results in gene-specific transcriptional upregulation

Farzaneh Modarresi[1], Mohammad Ali Faghihi[1], Miguel A Lopez-Toledano[2], Roya Pedram Fatemi[1], Marco Magistri[1], Shaun P Brothers[1], Marcel P van der Brug[2] & Claes Wahlestedt[1]

The ability to specifically upregulate genes *in vivo* holds great therapeutic promise. Here we show that inhibition or degradation of natural antisense transcripts (NATs) by single-stranded oligonucleotides or siRNAs can transiently and reversibly upregulate locus-specific gene expression. Brain-derived neurotrophic factor (BDNF) is normally repressed by a conserved noncoding antisense RNA transcript, *BDNF*-AS. Inhibition of this transcript upregulates *BDNF* mRNA by two- to sevenfold, alters chromatin marks at the *BDNF* locus, leads to increased protein levels and induces neuronal outgrowth and differentiation both *in vitro* and *in vivo*. We also show that inhibition of NATs leads to increases in glial-derived neurotrophic factor (GDNF) and ephrin receptor B2 (EPHB2) mRNA. Our data suggest that pharmacological approaches targeting NATs can confer locus-specific gene upregulation effects.

The number of noncoding RNAs in eukaryotic genomes increases as a function of developmental complexity[1,2]. In addition, there is a great deal of diversity of noncoding RNAs expressed in the nervous system[3,4]. Over the past few years, we and others have reported on functional natural antisense transcripts (NATs) and showed their potential involvement in human disorders, including Alzheimer's disease[5], Parkinson's disease[6] and Fragile X syndrome[7]. NATs typically originate opposite the sense strand of many protein-coding genes, often overlapping in part with mRNA, promoter and regulatory regions[8,9]. Multiple reports indicate that antisense transcripts are functional elements and use diverse transcriptional and post-transcriptional mechanisms to regulate gene expression (reviewed ref. 9). Previously, we showed that upregulation of CD97 coding mRNA can be attained by knockdown of its antisense RNA transcript[8]. Other reports indicated that siRNAs targeting promoter-derived noncoding RNAs caused upregulation of the progesterone receptor and other endogenous transcripts[10,11]. Transcriptional activation of *p21* (ref. 12) and the Oct4 promoter[13] were reported following NATs depletion. The existence of a human NAT that is transcribed opposite the gene encoding BDNF[14], a member of the 'neurotrophin' family of growth factors, has been reported[15]. Here we functionally characterize this antisense transcript in more detail.

Neurotrophins, such as BDNF, belong to a class of secreted growth factors that are essential for neuronal growth, maturation[16,17], differentiation and maintenance[18]. BDNF is also essential for neuronal plasticity[19–21] and has been shown to be involved in learning and memory processes[22]. BDNF is suggested to synchronize neuronal and glial maturation[23], participate in axonal and dendritic differentiation[24] and protect and enhance neuronal cell survival[25,26]. Neurotrophin expression levels are impaired in neurodegenerative[27–30] and in psychiatric and neurodevelopmental disorders[31–33]. The upregulation of neurotrophins is believed to have beneficial effects on several neurological disorders.

Here we characterize the role of *BDNF* antisense RNA (*BDNF*-AS, also annotated as *BDNF*-OS; nucleotide sequence of human *BDNF*-AS is provided in **Supplementary Data 1**), which we demonstrate regulates the expression of sense *BDNF* mRNA and protein, both *in vitro* and *in vivo*. We also show that glial-derived neurotrophic factor (*GDNF*) and ephrin receptor B2 (*EPHB2*) can be upregulated by blocking endogenous NATs. Our strategy for upregulation of mRNA expression uses antisense RNA transcript inhibitory molecules, which we term antagoNATs. We show that endogenous gene expression can be upregulated in a locus-specific manner by the removal or inhibition of NATs, which are transcribed from most transcriptional units[8,34]. Our study provides examples of functional noncoding RNAs that regulate protein output by altering chromatin structure, and we posit that this phenomenon is applicable to many other genomic loci.

RESULTS

Genomic organization of the human *BDNF* locus

Both *BDNF* mRNA and *BDNF*-AS display a complex splicing pattern; however, all variants share a common sense-antisense overlapping region[14,35]. The transcription start site of human *BDNF*-AS is located on the positive strand of chromosome 11 ~200 kb downstream from the *BDNF* mRNA promoter. Transcription from this site gives rise to 16–25 splice variants each containing six to eight exons[14]. Common to all these variants is exon 4, which does not overlap with *BDNF* mRNA, and exon 5, which contains 225 nucleotides of full complementarity to all 11 splice variants of *BDNF* mRNA (**Fig. 1a**). We searched our existing next-generation RNA sequencing data, which were

[1]Department of Psychiatry and Behavioral Sciences and Center for Therapeutic Innovation, John P. Hussman Institute for Human Genomics, University of Miami Miller School of Medicine, Miami, Florida, USA. [2]Present Addresses: Center for Molecular Biology and Biotechnology, Florida Atlantic University, Jupiter, Florida, USA (M.A.L.-T.) and Genentech Inc., S. San Francisco, California, USA (M.P.v.d.B.). Correspondence should be addressed to C.W. (cwahlestedt@med.miami.edu).

Received 29 September 2011; accepted 14 February 2012; published online 25 March 2012; doi:10.1038/nbt.2158

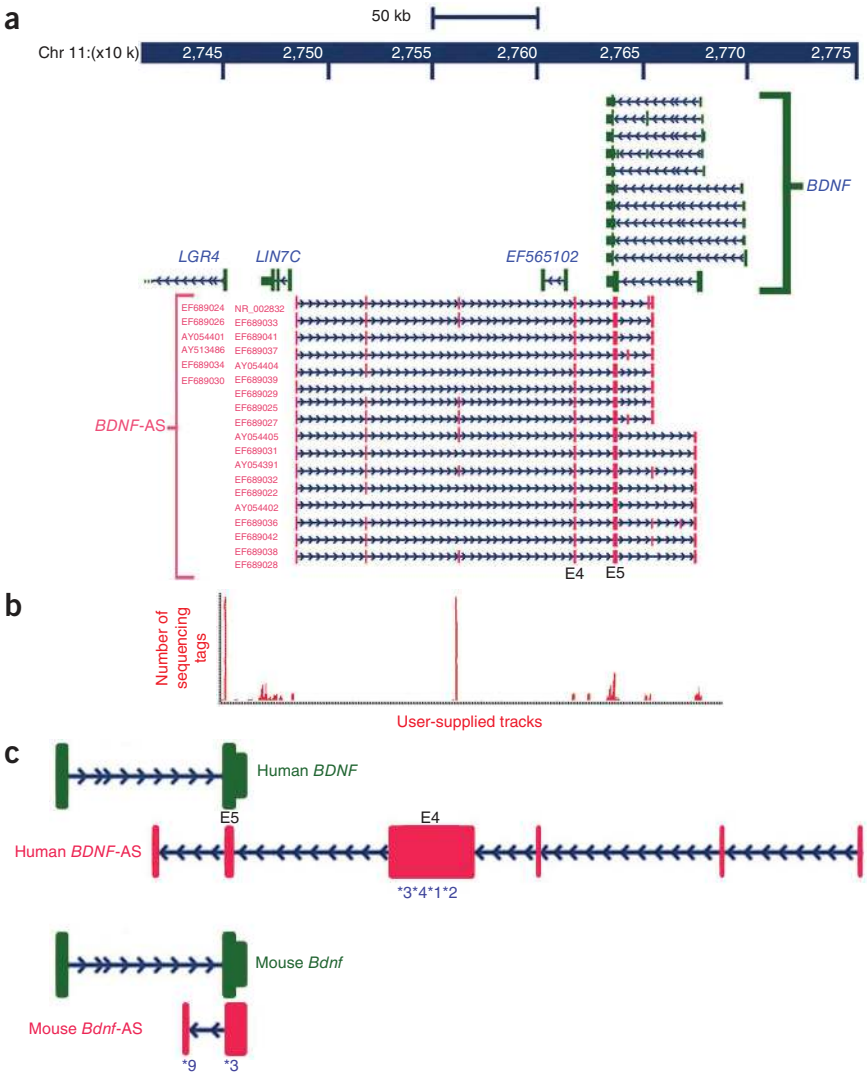

Figure 1 Genomic organization of the human *BDNF* locus. (**a**) Genomic location of the *BDNF* sense and antisense transcripts and their relation to the other neighboring genes on chromosome 11. Solid boxes show exons with arrows showing introns and the direction of transcription. Different splice variants of *BDNF*-AS transcript are transcribed from the opposite DNA strand as that of *BDNF* mRNA. All *BDNF*-AS splice variants have a common exon that overlaps with 225 bp of all variants of *BDNF* mRNA. (**b**) Sequence tags generated by next-generation sequencing from the human entorhinal cortex were aligned to the UCSC genome browser. Peaks represent number of sequencing tags, which represent nucleotide coverage, indicating reliable detection of *BDNF*-AS exons. (**c**) Identification of mouse *Bdnf*-AS by RACE experiments followed by sequencing. Proportional drawing representing human and mouse loci, showing direction of transcription for both sense and antisense transcripts, as well as the potential overlapping region. Mouse *Bdnf*-AS transcript is shorter than that of human and contains 1 or 2 exons. rtPCR primers, probes and siRNAs are designed to target the nonoverlapping parts of both transcripts. Blue asterisks and numbers below each denote target sites of siRNAs used in this study, as well as m*Bdnf*-antagoNAT3(*3) and m*Bdnf*-antagoNAT9 (*9).

generated from brain RNA samples on the Illumina platform, for the presence of *BDNF*-AS transcript (unpublished data). RNA deep sequencing data confirmed expression of *BDNF*-AS transcript in human brain RNA samples (**Fig. 1b**). Therefore, *BDNF*-AS has the potential to form an *in vivo* RNA-RNA duplex with *BDNF* mRNA through overlap of 225 complementary nucleotides.

Identification of mouse *Bdnf*-AS transcript

Although several human EST's have been reported to have the potential of forming sense-antisense pairs with *BDNF* transcripts[14,15], the mouse antisense *Bdnf* transcript has not previously been identified and thus *BDNF*-AS has erroneously been reported as a primate-specific transcript by others[35]. Using 5′ and 3′ rapid amplification of cDNA ends (RACE), we identified two mouse *Bdnf*-AS transcripts (**Fig. 1c**). Based on RACE data, we designed primers and probes for detection of mouse *Bdnf*-AS by real-time PCR (rtPCR). The combination of RACE experiments, followed by sequencing along with rtPCR, indicated the existence of a conserved noncoding antisense transcript to the mouse *Bdnf* mRNA. The mouse *Bdnf*-AS transcript has two splice variants containing 1 or 2 exons but both contain 934 nucleotides complementary to *Bdnf* mRNA (**Fig. 1c**). The nucleotide sequence of mouse *Bdnf*-AS is provided in **Supplementary Data 2**. Although the architectures of *BDNF*-AS in human and mouse are not entirely similar, the 225-bp overlapping region is almost identical between these two species (90% homology across the two species).

Expression analysis of *BDNF* and *BDNF*-AS

We measured the relative levels of *BDNF* and *BDNF*-AS transcripts in various human, monkey and mouse tissues by rtPCR and RNA fluorescence *in situ* hybridization (FISH). We also measured the absolute levels of *BDNF* and *BDNF*-AS transcripts by generating standard curves using DNA vectors containing cDNA of each transcript (**Supplementary Fig. 1**). In humans, *BDNF* mRNA levels are generally 10- to 100-fold higher than *BDNF*-AS transcript, except in the testis, kidney and heart, which contain equal or higher levels of *BDNF*-AS. Both transcripts are expressed in the brain, muscle and embryonic tissues (**Supplementary Fig. 2**). *BDNF* mRNA levels were relatively low in all post-natal tissues examined except in brain, bladder, heart and skeletal muscle (**Supplementary Fig. 3**). In rhesus monkeys (**Supplementary Fig. 4**) and mice (**Supplementary Figs. 5** and **6**), both transcripts are co-expressed in many tissues, which suggests *BDNF*-AS potential for regulation of *BDNF* mRNA.

Knockdown of *BDNF*-AS increases *BDNF in vitro*

To investigate the effect of antisense transcript degradation on sense expression levels, we designed three independent short interfering RNA (siRNA) molecules that targeted the nonoverlapping regions of the *BDNF*-AS transcript (**Fig. 1b** and **Supplementary Table 1**). Transfection of these siRNAs into several human and mouse cell lines, including HEK293T cells, resulted in >85% knockdown of the *BDNF*-AS transcript, accompanied by a two- to fivefold upregulation of the *BDNF* transcript (**Fig. 2a**). The upregulation of *BDNF* mRNA was not related to the choice of endogenous controls (**Supplementary Fig. 7**).

Control reactions that did not include reverse transcriptase or template did not yield any product, suggesting that our rtPCR reactions reliably detected the transcript and was not contaminated by genomic DNA. Additionally, we tested the final PCR products for each set of primers and probe on a gel to ensure that only one product was amplified (**Supplementary Fig. 8**).

To monitor the sequential events after administration of *BDNF*-AS-targeted siRNA, we treated HEK293T cells with *BDNF*-AS-targeting siRNA, and measured the endogenous expression of both *BDNF* mRNA and *BDNF*-AS transcripts at several time points (**Fig. 2b**). We observed downregulation of *BDNF*-AS at 6 h with maximum efficacy between 24 and 48 h and lasting up to 72 h (**Fig. 2b**). Upregulation of *BDNF* mRNA started 18 h after transfection and reached the maximum at 48 h then decreased at 72 h before returning to pretreatment levels by 96 h. These data show that a transient knockdown of NAT levels leads to a fully reversible increase in *BDNF* mRNA levels.

Moreover, we examined BDNF protein levels by enzyme-linked immunosorbent analysis (ELISA) after treating HEK293T cells with two active *BDNF*-AS siRNAs, control siRNA or scrambled siRNAs (**Fig. 2c**). We also measured BDNF protein level by western blot analysis following transfection of cells with *BDNF*-AS siRNA-1 or control siRNA (**Fig. 2d**). Both ELISA (**Fig. 2c**) and western blot analysis (**Fig. 2d**) experiments demonstrated that treatment of cells with siRNA targeting *BDNF*-AS considerably increased the expression of BDNF protein. We observed that the magnitude of BDNF protein upregulation (about twofold) was less than the extent of mRNA upregulation (two- to sevenfold). This suggests that protein upregulation is stoichiometrically discordant with mRNA in these cells, especially considering that one molecule of mRNA often produces more than one molecule of protein. Post-transcriptional regulatory mechanisms, such as microRNAs, may account for this potential discrepancy in BDNF protein output[36–38] (**Supplementary Fig. 9**).

BDNF-AS did not alter *BDNF* sense-RNA stability

To examine the effects of *BDNF*-AS transcripts on the stability of *BDNF* sense transcripts, we depleted *BDNF*-AS with siRNA and then treated cells with α-amanitin, an inhibitor of RNA polymerase II. We found that the baseline half-life for *BDNF*-AS was 15.3 h, nearly 3 h longer than that of the *BDNF* sense transcript (**Supplementary Fig. 10**). There was no detectable change in *BDNF* sense-RNA stability after reduction of *BDNF*-AS transcript, suggesting that unlike highly abundant antisense transcripts[5], *BDNF*-AS does not alter *BDNF* sense-mRNA stability. Recently it has been suggested that some NATs can produce endogenous siRNAs from the overlapping region between sense and antisense RNAs. However, none of the endogenous siRNAs previously identified[39] in mouse oocytes originated from the *Bdnf* locus.

Targeting of *BDNF*-AS by antagoNATs

Having established that antisense transcripts play a key role in regulating the expression levels of sense transcripts, we sought to test an alternate, simpler way to relieve the inhibitory effects of NATs. We introduce the term antagoNAT here to describe a single-stranded modified DNA or RNA oligonucleotide that inhibits the activity of antisense transcript. We hypothesized that the use of antagoNATs should have a similar outcome on *BDNF* expression as observed with *BDNF*-AS siRNA. To test this hypothesis, we designed a set of oligonucleotides tiling the entire region of overlap between human *BDNF*-AS and *BDNF*. For these experiments, each antagoNAT was a 14-nucleotide oligonucleotide containing a mixture of 2′-*O*-methyl RNA and locked nucleic acid (LNA) modifications (Online Methods). We found several efficacious antagoNATs capable of upregulating *BDNF* mRNA. h*BDNF*-antagoNAT1 and h*BDNF*-antagoNAT4, which both target the first part of the overlapping region, produced the largest response (**Supplementary Fig. 11**). Our data suggest that blockage of *BDNF* antisense RNA, by single-stranded antagoNATs, is sufficient in causing an increase in *BDNF* mRNA.

To see if this method was applicable in different species, we designed single-stranded, 16-nucleotide gapmers[40] consisting of three LNA-modified DNA bases at each of the ends with ten unmodified DNA bases in the middle, allowing for RNaseH cleavage. Two antagoNATs (m*Bdnf*-antagoNAT3 and m*Bdnf*-antagoNAT9)

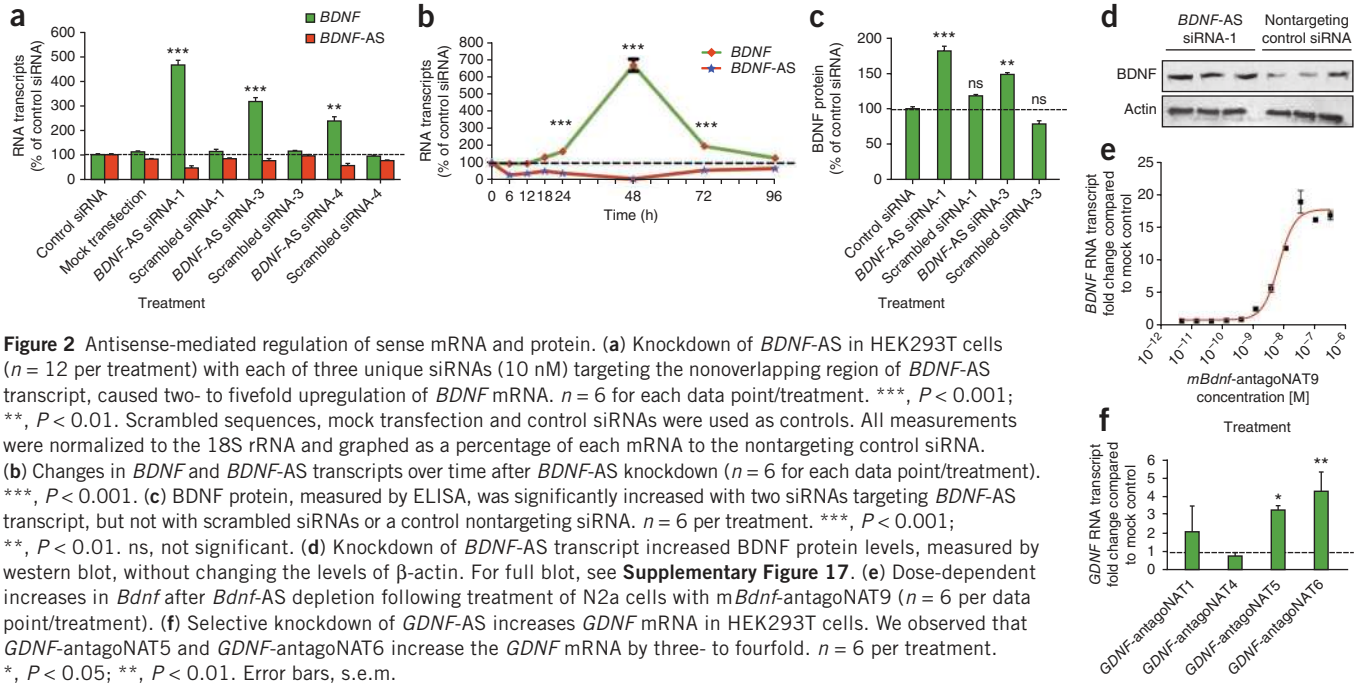

Figure 2 Antisense-mediated regulation of sense mRNA and protein. (**a**) Knockdown of *BDNF*-AS in HEK293T cells ($n = 12$ per treatment) with each of three unique siRNAs (10 nM) targeting the nonoverlapping region of *BDNF*-AS transcript, caused two- to fivefold upregulation of *BDNF* mRNA. $n = 6$ for each data point/treatment. ***, $P < 0.001$; **, $P < 0.01$. Scrambled sequences, mock transfection and control siRNAs were used as controls. All measurements were normalized to the 18S rRNA and graphed as a percentage of each mRNA to the nontargeting control siRNA. (**b**) Changes in *BDNF* and *BDNF*-AS transcripts over time after *BDNF*-AS knockdown ($n = 6$ for each data point/treatment). ***, $P < 0.001$. (**c**) BDNF protein, measured by ELISA, was significantly increased with two siRNAs targeting *BDNF*-AS transcript, but not with scrambled siRNAs or a control nontargeting siRNA. $n = 6$ per treatment. ***, $P < 0.001$; **, $P < 0.01$. ns, not significant. (**d**) Knockdown of *BDNF*-AS transcript increased BDNF protein levels, measured by western blot, without changing the levels of β-actin. For full blot, see **Supplementary Figure 17**. (**e**) Dose-dependent increases in *Bdnf* after *Bdnf*-AS depletion following treatment of N2a cells with m*Bdnf*-antagoNAT9 ($n = 6$ per data point/treatment). (**f**) Selective knockdown of *GDNF*-AS increases *GDNF* mRNA in HEK293T cells. We observed that *GDNF*-antagoNAT5 and *GDNF*-antagoNAT6 increase the *GDNF* mRNA by three- to fourfold. $n = 6$ per treatment. *, $P < 0.05$; **, $P < 0.01$. Error bars, s.e.m.

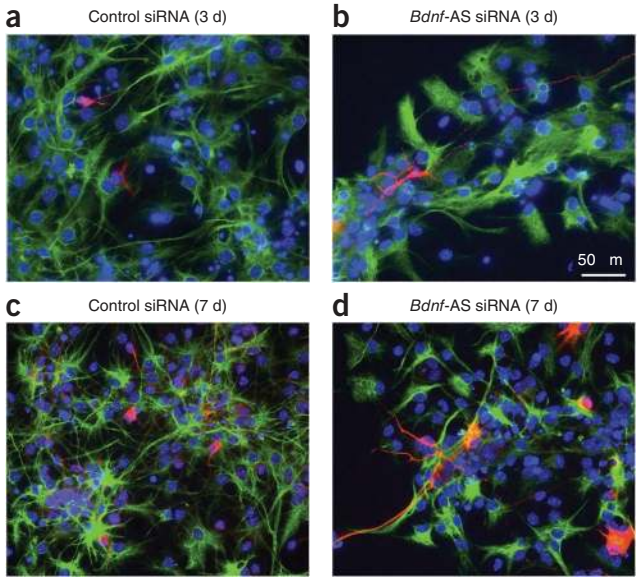

Figure 3 *Bdnf* upregulation increases neuronal outgrowth. (**a**,**b**) Immunocytochemistry images of hippocampal neurospheres treated with either control siRNA (**a**) or *Bdnf*-AS siRNA (**b**) 3 d after plating. (**c**,**d**) Immunocytochemistry images of neuronal maturation and neurite outgrowth in hippocampal neurospheres treated with either control siRNA (**c**) or *Bdnf*-AS siRNA (**d**) 7 d after plating. Treatment of cells with siRNA targeting the *Bdnf*-AS transcript resulted in increased neuronal cell number as well as increase in neurite outgrowth and maturation, both at 3 d and 7 d after plating neurospheres. Red, β-tubulin III; green, GFAP; DAPI, blue.

consistently showed a statistically significant ($P < 0.001$, two-way ANOVA) increase in *Bdnf* mRNA levels in mouse N2a cells (**Supplementary Fig. 12**). To establish an optimal dosage for further *in vitro* studies, we performed concentration-response experiments with 11 different concentrations (1:3 serial dilutions ranging from 300 nM to 5 pM) of m*Bdnf*-antagoNAT9, measuring fold changes in *Bdnf* mRNA levels (**Fig. 2e**). *Bdnf* mRNA levels increased with increasing concentrations of m*Bdnf*-antagoNAT9 from 1–300 nM resulting in an EC_{50} of 6.6 nM.

Knockdown of *GDNF*-AS increases *GDNF* mRNA *in vitro*

To examine whether antagoNATs could be used to upregulate other genes, we designed several antagoNATs targeting the *GDNF* antisense transcript, a low-abundance noncoding antisense RNA that overlaps with the sense transcript. We found two antagoNATs that increased the *GDNF* mRNA by three- to fourfold (**Fig. 2f**). To help determine whether the effects were specific to nerve growth factor genes, or were perhaps applicable to a larger number of genes, we also used antagoNATs to target antisense transcripts of the ephrin type-B receptor 2 (*EPHB2*) gene, resulting in upregulation of *EPHB2* mRNA in HEK293T cells (**Supplementary Fig. 13**).

Bdnf upregulation increases neuronal outgrowth

It is well established that BDNF stimulates neuronal outgrowth and adult neurogenesis[41,42]. Therefore, to demonstrate that our strategy for upregulating gene expression can lead to functional consequences, we treated neurospheres with siRNA against *Bdnf*-AS then determined the effects on neurite outgrowth. We found that an increase in endogenous *Bdnf* due to the knockdown of *Bdnf*-AS transcript resulted in increased neurite outgrowth and maturation (**Fig. 3a–d**). These data suggest that the upregulation of endogenous *Bdnf*, due to inhibition of antisense RNA, induces neuronal differentiation in neuronal progenitor cells.

Knockdown of *Bdnf*-AS increases *Bdnf in vivo*

We used osmotic mini-pumps for intracerebroventricular delivery of m*Bdnf*-antagoNAT9 to C57BL/6 mice. We selected m*Bdnf*-antagoNAT9, which targets a nonoverlapping region of mouse *Bdnf*-AS, over other active antagoNATs because it increases *Bdnf* mRNA *in vitro* efficaciously. After 28 d of continuous antagoNAT infusion, *Bdnf* mRNA levels were increased across forebrain regions adjacent to the third ventricle in mice treated with m*Bdnf*-antagoNAT9 as compared to a control oligonucleotide (**Fig. 4a**,**b**). *Bdnf* mRNA and *Bdnf*-AS transcripts were unaltered in the hypothalamus, a structure that is not immediately adjacent to the third ventricle (**Fig. 4c**). Moreover, we find that antagoNAT-mediated blockade of *Bdnf*-AS results in increased Bdnf protein levels (**Fig. 4d**,**e**). These findings correspond with the *in vitro* data described above and indicate that the blockade of *Bdnf*-AS results in the increase of *Bdnf* mRNA and protein expression *in vivo*.

We injected BrdU in the mice treated with m*Bdnf*-antagoNAT9 in the first week of the study for 5 d. After 28 d of continuous antagoNAT infusion, we performed histological examination of brain tissues and quantified neuronal proliferation and survival using Ki67 and BrdU markers, respectively. In mice treated with m*Bdnf*-antagoNAT9, we observed an increase in cells expressing Ki67 (a marker of cell proliferation) as compared with control mice (**Fig. 5a**,**b**). We quantified the number of Ki67-positive cells and found an increase in mice treated with m*Bdnf*-antagoNAT9 compared with control oligonucleotide (**Fig. 5c**). In mice treated with m*Bdnf*-antagoNAT9, there was a significant increase in BrdU incorporation (surviving cells) as compared with the control oligonucleotide-treated

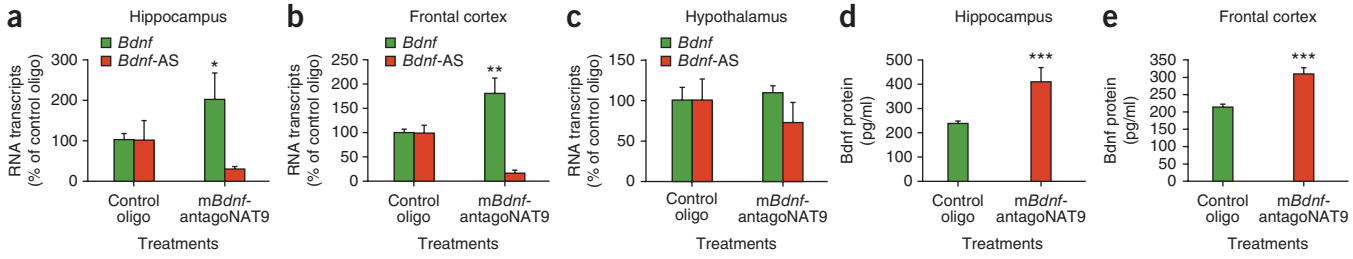

Figure 4 *Bdnf*-AS regulates *Bdnf* mRNA and protein *in vivo*. (**a**–**c**) Infusion of m*Bdnf*-antagoNAT9 (CAACATATCAGGAGCC), but not a control oligonucleotide (CCACGCGCAGTACATG), resulted in an increase in *Bdnf* levels in the hippocampus (**a**) and frontal cortex (**b**); in the hypothalamus (**c**) both transcripts were unchanged. $n = 5$ per treatment group. (**d**,**e**) We assessed Bdnf protein levels by ELISA and found that m*Bdnf*-antagoNAT9 treatment results in an increase in Bdnf protein, both in the hippocampus (**d**) and frontal cortex (**e**), as compared to control oligonucleotide-treated mice. Error bars, s.e.m. *, $P < 0.05$; **, $P < 0.01$; ***, $P < 0.001$.

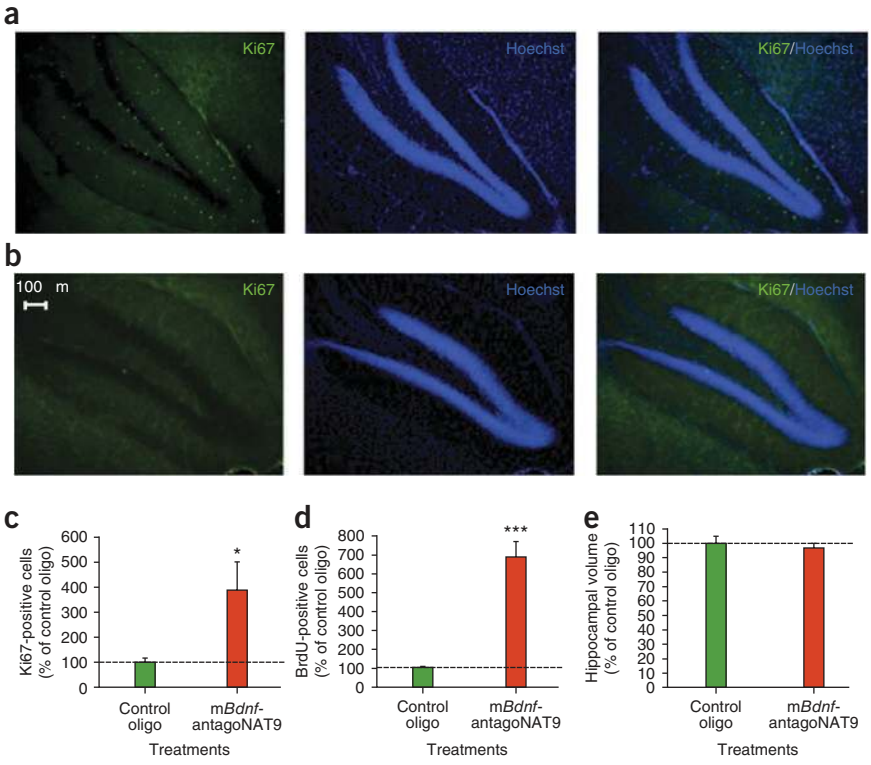

Figure 5 Blocking of *Bdnf*-AS, *in vivo*, causes an increase in neuronal survival and proliferation. (**a**,**b**) Brain tissue of mice treated with m*Bdnf*-antagoNAT9 (**a**) or control oligos (**b**). Increase observed in Ki67-positive (proliferating) cells in mice receiving m*Bdnf*-antagoNAT treatment compared to mice receiving control oligos. In mice treated with m*Bdnf*-antagoNAT9 (**a**), there was an increase in proliferating cells, as compared to control-treated mice (**b**). (**c**) Mice treated with m*Bdnf*-antagoNAT9 had a significant increase in the number of Ki67-positive cells as compared to control-treated mice. (**d**) In mice treated with m*Bdnf*-antagoNAT9, there was a significant increase in the number of surviving cells (BrdU-positive) as compared to control oligonucleotide treated mice. (**e**) There were no differences in hippocampal volume between control and m*Bdnf*-antagoNAT9-treated mice. $n = 5$ per treatment group. *, $P < 0.05$; ***, $P < 0.001$. Error bars, s.e.m.

mice (**Fig. 5d**). There were no differences in hippocampal volume between control and m*Bdnf*-antagoNAT9 treated mice (**Fig. 5e**). These findings demonstrate that *Bdnf*-AS regulates *Bdnf* levels *in vivo*.

Locus-specific effects of *BDNF*-AS degradation

To validate the specificity of the *BDNF*-AS targeting siRNA and to show locus-specific effects of antisense reduction, we performed rtPCR and found that the knockdown of *BDNF*-AS transcript increases *BDNF* mRNA without any effects on neurotrophic tyrosine kinase receptor type 2 (*TrkB*), a receptor for BDNF, or on neighboring genes (*LIN7C* and *KIF18A*) in both directions (**Supplementary Fig. 14**).

BDNF-AS induces repressive chromatin marks

We hypothesized that *BDNF*-AS regulates *BNDF* mRNA transcript levels by regulating epigenetic marks. As such, we measured the association of repressive (H3K9met3 and H3K27met3) and active (H3K4met3 and H3K36met3) chromatin marks at the *BDNF* genomic locus (**Fig. 6a**). After depleting *BDNF*-AS by siRNA, we performed chromatin immunoprecipitation (ChIP) assays. We designed 16 primers to span the entire 270-kb region extending through to the neighboring

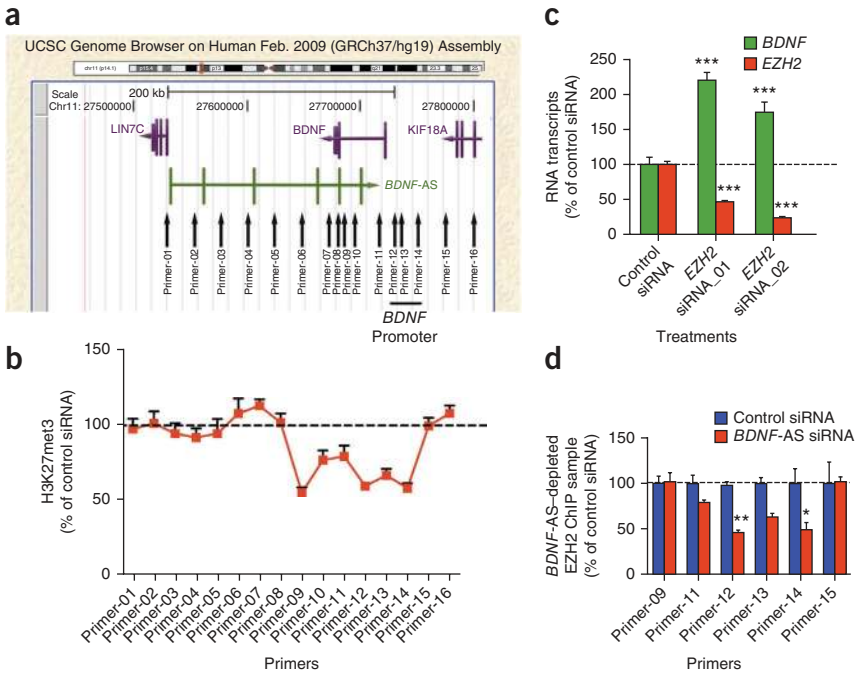

Figure 6 Removal of *BDNF*-AS resulted in the modification of chromatin marks. (**a**) HEK293T cells were treated with control or *BDNF*-AS siRNA followed by Immunoprecipitation and DNA extraction. DNA samples were analyzed using 16 primer sets covering the entire *BDNF* gene locus, and the *BDNF* promoter region, as indicated in the imposed image on UCSC genome browser. (**b**) Decrease in association of the repressive chromatin marker, H3K27me3, upon treatment of the cells with *BDNF*-AS siRNA, both at the sense-antisense overlapping (primer 9) and promoter (primer 12–14) regions ($n = 6$ for each data point). The observed chromatin modification did not extend toward neighboring genes. (**c**) Knockdown of *EZH2*, by either one of two different siRNAs, mimics or phenocopies the *BDNF*-AS knockdown and causes upregulation of *BDNF* mRNA. $n = 6$ for each data point/treatment. ***, $P < 0.001$. (**d**) ChIP assay with EZH2 antibody shows decrease in EZH2 association with the *BDNF* promoter upon depletion of the *BDNF*-AS transcript by siRNA. Not all 16 primer sets gave detectable PCR signals. $n = 6$ for each data point/treatment. **, $P < 0.01$; *, $P < 0.05$. Error bars, s.e.m.

genes *LIN7C* and *KIF18A*. We studied the immunoprecipitated DNA using individual primer sets using rtPCR and we found that the siRNA-mediated depletion of the *BDNF*-AS transcript caused reduction in H3K27me3 association in both the sense-antisense overlapping region, indicated by primer set 9, and in the upstream *BDNF* promoter region (**Fig. 6b**). We found similar reduction in H3K27me3 binding to the promoter of the mouse *Bdnf* gene upon treatment of N2a cells with m*Bdnf*-antagoNAT9 (**Supplementary Fig. 15**). Furthermore, we found that alterations in repressive marks were specific to H3K27me3, as we were not able to detect notable changes in H3K9me3, H3K4me3 and H3K36me3 (**Supplementary Fig. 16**). These data suggest that *BDNF*-AS might play a role in the guidance, introduction and maintenance of H3K27me3 at the *BDNF* locus.

EZH2 is a histone lysine methyltransferase largely responsible for the addition of the repressive mark, H3K27me3 (ref. 43). We observed that the ablation of EZH2 activity using two different siRNAs produced the same phenotype as the *BDNF*-AS knockdown and caused upregulation of *BDNF* mRNA (**Fig. 6c**). After treating cells with *BDNF*-AS siRNA, we used ChIP to track changes in EZH2 binding to the *BDNF* locus and observed a reduction in EZH2 binding at the *BDNF* promoter (**Fig. 6d**). However, not all 16 primer sets gave detectable PCR signals, which could be attributed to the lack of direct binding of EZH2 to chromatin. Given the reduced presence of EZH2 and the loss of the H3K27me3 at the *BDNF* promoter when *BDNF*-AS is knocked down, we conclude that *BDNF*-AS inhibits *BDNF* mRNA transcription by recruiting EZH2 and likely other members of the polycomb repressive complex 2 (PRC2) to the *BDNF* promoter region. Removal or inhibition of *BDNF*-AS could lead to the locus-specific upregulation of *BDNF* mRNA and protein.

DISCUSSION

NATs, likely for a host of different genes, can be manipulated to obtain locus-specific alteration in chromatin modification and therefore gene expression. How might low copy number NATs exert such a wide range of effects? It is becoming apparent that antisense RNA molecules exert local effects by maintaining or modifying chromatin structure, ultimately activating or suppressing sense gene expression[9,44]. As examples, we show here that cleavage or inhibition of the antisense transcripts of *BDNF*, *GDNF* and *EPHB2* genes leads to the upregulation of corresponding mRNAs. In the context of the work presented here, antagoNATs could be used as a therapeutic strategy to inhibit *BDNF*-AS and consequently enhance neuronal proliferation and survival in a variety of disease states. Upregulating the endogenous *BDNF* gene, with this strategy, may result in the production of RNA molecules that contain all natural modifications and represent relevant spliced isoforms. Further studies will be required to evaluate the merits of this approach versus administering synthetic BDNF molecules, for example.

We propose that EZH2, and likely the entire PRC2 complex, is necessary for the action of *BDNF*-AS and other similar NATs. Along with EZH2, at least three other proteins (EED, SUZ12 and RBAP48) are known to make up the core components of PRC2. Recent studies provide evidence for direct RNA-protein interaction between EZH2 and many noncoding RNA transcripts[45]. Studies of X-chromosome inactivation[46] and the HOX gene cluster[47] show that RNA transcripts are involved in the PRC2-mediated induction of H3K27me3 repressive chromatin marks. Over 9,000 RNA molecules, many of them antisense RNA transcripts interact with PRC2 in embryonic stem cells[45]. Epigenetic silencing of *p15* and *DM1* are reported to involve heterochromatin formation by its antisense RNA[48,49]. How the NAT and EZH2/PRC2 components interact remains to be investigated; however, targeting NAT-EZH2 interaction might have therapeutic implications, especially for neurodegenerative disorders, where the upregulation of BDNF is desirable.

METHODS

Methods and any associated references are available in the online version of the paper at http://www.nature.com/naturebiotechnology/.

Note: Supplementary information is available on the Nature Biotechnology website.

ACKNOWLEDGMENTS

Q.-R. Liu from the National Institute of Drug Abuse kindly provided us with constructs that contain three splice variants of the human *BDNF*-AS transcript. We thank C. Coito, P. Frost, J. Hsiao and O. Khorkova at OPKO-CURNA for helpful discussions. The US National Institutes of Health (5R01NS063974 and 5RC2AG036596) funded this work. A significant portion of this study was carried out when the investigators were employed at The Scripps Research Institute and/or the Karolinska Institutet.

AUTHOR CONTRIBUTIONS

F.M., M.A.F., M.A.L.-T., R.P.F. and M.M. each contributed experimental data to this work. M.P.v.d.B. performed RNA deep sequencing of brain samples. F.M., M.A.F., M.A.L.-T., R.P.F., M.M., S.P.B. and C.W. all contributed to the concepts behind the work; each were also responsible for contributions to the text of this article.

COMPETING FINANCIAL INTERESTS

The authors declare competing financial interests: details accompany the full-text HTML version of the paper at http://www.nature.com/naturebiotechnology/.

Published online at http://www.nature.com/naturebiotechnology/.
Reprints and permissions information is available online at http://www.nature.com/reprints/index.html.

1. Mehler, M.F. & Mattick, J.S. Non-coding RNAs in the nervous system. *J. Physiol. (Lond.)* **575**, 333–341 (2006).
2. Mattick, J.S. & Makunin, I.V. Non-coding RNA. *Hum. Mol. Genet.* **15** Spec No 1, R17–R29 (2006).
3. Bernard, D. *et al.* A long nuclear-retained non-coding RNA regulates synaptogenesis by modulating gene expression. *EMBO J.* **29**, 3082–3093 (2010).
4. Mercer, T.R., Dinger, M.E., Sunkin, S.M., Mehler, M.F. & Mattick, J.S. Specific expression of long noncoding RNAs in the mouse brain. *Proc. Natl. Acad. Sci. USA* **105**, 716–721 (2008).
5. Faghihi, M.A. *et al.* Expression of a noncoding RNA is elevated in Alzheimer's disease and drives rapid feed-forward regulation of beta-secretase. *Nat. Med.* **14**, 723–730 (2008).
6. Scheele, C. *et al.* The human PINK1 locus is regulated *in vivo* by a non-coding natural antisense RNA during modulation of mitochondrial function. *BMC Genomics* **8**, 74 (2007).
7. Khalil, A.M., Faghihi, M.A., Modarresi, F., Brothers, S.P. & Wahlestedt, C. A novel RNA transcript with antiapoptotic function is silenced in fragile x syndrome. *PLoS ONE* **3**, e1486 (2008).
8. Katayama, S. *et al.* Antisense transcription in the mammalian transcriptome. *Science* **309**, 1564–1566 (2005).
9. Faghihi, M.A. & Wahlestedt, C. Regulatory roles of natural antisense transcripts. *Nat. Rev. Mol. Cell Biol.* **10**, 637–643 (2009).
10. Janowski, B.A. *et al.* Activating gene expression in mammalian cells with promoter-targeted duplex RNAs. *Nat. Chem. Biol.* **3**, 166–173 (2007).
11. Watts, J.K. *et al.* Effect of chemical modifications on modulation of gene expression by duplex antigene RNAs that are complementary to non-coding transcripts at gene promoters. *Nucleic Acids Res.* **38**, 5242–5259 (2010).
12. Morris, K.V., Santoso, S., Turner, A.M., Pastori, C. & Hawkins, P.G. Bidirectional transcription directs both transcriptional gene activation and suppression in human cells. *PLoS Genet.* **4**, e1000258 (2008).
13. Hawkins, P.G. & Morris, K.V. Transcriptional regulation of Oct4 by a long non-coding RNA antisense to Oct4-pseudogene 5. *Transcription* **1**, 165–175 (2010).
14. Pruunsild, P., Kazantseva, A., Aid, T., Palm, K. & Timmusk, T. Dissecting the human BDNF locus: bidirectional transcription, complex splicing, and multiple promoters. *Genomics* **90**, 397–406 (2007).
15. Liu, Q.R. *et al.* Human brain derived neurotrophic factor (BDNF) genes, splicing patterns, and assessments of associations with substance abuse and Parkinson's disease. *Am. J. Med. Genet.* **134**, 93–103 (2005).
16. Hasbi, A. *et al.* Calcium signaling cascade links dopamine D1–D2 receptor heteromer to striatal BDNF production and neuronal growth. *Proc. Natl. Acad. Sci. USA* **106**, 21377–21382 (2009).
17. Trzaska, K.A. *et al.* Brain-derived neurotrophic factor facilitates maturation of mesenchymal stem cell-derived dopamine progenitors to functional neurons. *J. Neurochem.* **110**, 1058–1069 (2009).

18. Yoshimura, R., Ito, K. & Endo, Y. Differentiation/maturation of neuropeptide Y neurons in the corpus callosum is promoted by brain-derived neurotrophic factor in mouse brain slice cultures. *Neurosci. Lett.* **450**, 262–265 (2009).
19. Antal, A. *et al.* Brain-derived neurotrophic factor (BDNF) gene polymorphisms shape cortical plasticity in humans. *Brain Stimulat.* **3**, 230–237 (2010).
20. Castillo, D.V. & Escobar, M.L. A role for MAPK and PI-3K signaling pathways in brain-derived neurotrophic factor modification of conditioned taste aversion retention. *Behav. Brain Res.* **217**, 248–252 (2011).
21. Nikolakopoulou, A.M., Meynard, M.M., Marshak, S. & Cohen-Cory, S. Synaptic maturation of the *Xenopus* retinotectal system: effects of brain-derived neurotrophic factor on synapse ultrastructure. *J. Comp. Neurol.* **518**, 972–989 (2010).
22. Choi, D.C. *et al.* Prelimbic cortical BDNF is required for memory of learned fear but not extinction or innate fear. *Proc. Natl. Acad. Sci. USA* **107**, 2675–2680 (2010).
23. Ortega, J.A. & Alcantara, S. BDNF/MAPK/ERK-induced BMP7 expression in the developing cerebral cortex induces premature radial glia differentiation and impairs neuronal migration. *Cereb. Cortex* **20**, 2132–2144 (2010).
24. Chapleau, C.A., Larimore, J.L., Theibert, A. & Pozzo-Miller, L. Modulation of dendritic spine development and plasticity by BDNF and vesicular trafficking: fundamental roles in neurodevelopmental disorders associated with mental retardation and autism. *J. Neurodev. Disord.* **1**, 185–196 (2009).
25. Wu, S.Y. *et al.* Running exercise protects the substantia nigra dopaminergic neurons against inflammation-induced degeneration via the activation of BDNF signaling pathway. *Brain Behav. Immun.* **25**, 135–146 (2011).
26. Yang, L.C. *et al.* Extranuclear estrogen receptors mediate the neuroprotective effects of estrogen in the rat hippocampus. *PLoS ONE* **5**, e9851 (2010).
27. Laske, C. *et al.* Higher BDNF serum levels predict slower cognitive decline in Alzheimer's disease patients. *Int. J. Neuropsychopharmacol.* **14**, 399–404 (2011).
28. Zeng, Y., Zhao, D. & Xie, C.W. Neurotrophins enhance CaMKII activity and rescue amyloid-beta-induced deficits in hippocampal synaptic plasticity. *J. Alzheimers Dis.* **21**, 823–831 (2010).
29. Frade, J.M. & Lopez-Sanchez, N. A novel hypothesis for Alzheimer's disease based on neuronal tetraploidy induced by p75(NTR). *Cell Cycle* **9**, 1934–1941 (2010).
30. Massa, S.M. *et al.* Small-molecule BDNF mimetics activate TrkB signaling and prevent neuronal degeneration in rodents. *J. Clin. Invest.* **120**, 1774–1785 (2010).
31. Luo, K.R. *et al.* Differential regulation of neurotrophin S100B and BDNF in two rat models of depression. *Prog. Neuropsychopharmacol. Biol. Psychiatry* **34**, 1433–1439 (2010).
32. Gonul, A.S. *et al.* Association of the brain-derived neurotrophic factor Val66Met polymorphism with hippocampus volumes in drug-free depressed patients. *World J. Biol. Psychiatry* **12**, 110–118 (2011).
33. Dell'Osso, L. *et al.* Associations between brain-derived neurotrophic factor plasma levels and severity of the illness, recurrence and symptoms in depressed patients. *Neuropsychobiology* **62**, 207–212 (2010).
34. He, Y., Vogelstein, B., Velculescu, V.E., Papadopoulos, N. & Kinzler, K.W. The antisense transcriptomes of human cells. *Science* **322**, 1855–1857 (2008).
35. Liu, Q.R. *et al.* Rodent BDNF genes, novel promoters, novel splice variants, and regulation by cocaine. *Brain Res.* **1067**, 1–12 (2006).
36. Abuhatzira, L., Makedonski, K., Kaufman, Y., Razin, A. & Shemer, R. MeCP2 deficiency in the brain decreases BDNF levels by REST/CoREST-mediated repression and increases TRKB production. *Epigenetics* **2**, 214–222 (2007).
37. Ogier, M. *et al.* Brain-derived neurotrophic factor expression and respiratory function improve after ampakine treatment in a mouse model of Rett syndrome. *J. Neurosci.* **27**, 10912–10917 (2007).
38. Klein, M.E. *et al.* Homeostatic regulation of MeCP2 expression by a CREB-induced microRNA. *Nat. Neurosci.* **10**, 1513–1514 (2007).
39. Watanabe, T. *et al.* Endogenous siRNAs from naturally formed dsRNAs regulate transcripts in mouse oocytes. *Nature* **453**, 539–543 (2008).
40. Wahlestedt, C. *et al.* Potent and nontoxic antisense oligonucleotides containing locked nucleic acids. *Proc. Natl. Acad. Sci. USA* **97**, 5633–5638 (2000).
41. Park, H.R. *et al.* A high-fat diet impairs neurogenesis: involvement of lipid peroxidation and brain-derived neurotrophic factor. *Neurosci. Lett.* **482**, 235–239 (2010).
42. Im, S.H. *et al.* Induction of striatal neurogenesis enhances functional recovery in an adult animal model of neonatal hypoxic-ischemic brain injury. *Neuroscience* **169**, 259–268 (2010).
43. Chase, A. & Cross, N.C. Aberrations of EZH2 in cancer. *Clin. Cancer Res.* **17**, 2613–2618 (2011).
44. Morris, K.V. Long antisense non-coding RNAs function to direct epigenetic complexes that regulate transcription in human cells. *Epigenetics* **4**, 296–301 (2009).
45. Zhao, J. *et al.* Genome-wide identification of polycomb-associated RNAs by RIP-seq. *Mol. Cell* **40**, 939–953 (2010).
46. Zhao, J., Sun, B.K., Erwin, J.A., Song, J.J. & Lee, J.T. Polycomb proteins targeted by a short repeat RNA to the mouse X chromosome. *Science* **322**, 750–756 (2008).
47. Rinn, J.L. *et al.* Functional demarcation of active and silent chromatin domains in human HOX loci by noncoding RNAs. *Cell* **129**, 1311–1323 (2007).
48. Yu, W. *et al.* Epigenetic silencing of tumour suppressor gene p15 by its antisense RNA. *Nature* **451**, 202–206 (2008).
49. Cho, D.H. *et al.* Antisense transcription and heterochromatin at the DM1 CTG repeats are constrained by CTCF. *Mol. Cell* **20**, 483–489 (2005).

ONLINE METHODS

Mouse studies. We obtained approval for mouse studies from the Institutional Animal Care and Use Committee at The Scripps Research Institute, where the animal experiments were performed. We used 10 eight-week-old male C57BL/6 mice for *in vivo* experiments. We prepared mice with chronic indwelling cannulae in the dorsal third ventricle implanted subcutaneously with osmotic mini-pumps that delivered continuous infusions (0.11 µl/h) of synthetic antisense oligonucleotide directed against *Bdnf*-AS (m*Bdnf*-antagoNAT9) or control oligonucleotide (inert sequence (CCACGCGCAGTACATG) that does not exist in human or mouse at a dose of 1.5 mg/kg/d for 4 weeks. We connected tubing to the exit port of the osmotic mini-pump and tunneled it subcutaneously to the indwelling cannula, such that the treatments were delivered directly into the brain. At 5 d after implantation all animals received daily intraperitoneal injection of BrdU (80 mg/kg) for five consecutive days. At 28 d after surgery, we euthanized the animals and excised three tissues (hippocampus, frontal cortex and hypothalamus) from each mouse brain for quantitative RNA measurements.

Design of modified antagoNAT molecules. We designed and tested a number of DNA-based antisense oligonucleotides, termed antagoNATs, targeting noncoding *Bdnf*-AS and other antisense transcripts. We designed various antagoNATs ranging from 12 to 20 nucleotides in length with or without full phosphorothioate modification plus/minus 2′-*O*-methyl RNA or LNA-modified nucleotides. We observed the highest efficacy on *Bdnf* mRNA levels with 16-nucleotide phosphorothioate gapmer with three LNA-modified nucleotides[40] at each end (XXXnnnnnnnnnnXXX). For blocking interactions between human *BDNF* sense-antisense transcripts, we used 14-nucleotide oligonucleotide containing both LNA and 2′-*O*-methyl RNA molecules. Although these 2′-*O*-methyl RNA-modified oligonucleotides are suggested to only block the RNA, we observed marginal downregulation of targeted RNAs in this experiment (**Supplementary Fig. 12**). Sequences of various antagoNATs, as well as all other siRNAs, primers and probes used for these studies are listed in **Supplementary Table 1**.

RACE. Sequence information for the potential mouse *Bdnf*-AS was retrieved from the UCSC Genome Bioinformatics web site. Using RACE-ready cDNA (Ambion) from the mouse brain we amplified the 5′ and 3′ ends of *Bdnf*-AS by nested PCR with gene specific and kit primers. Alternatively, using 250 ng poly(A) RNA from the testis as starting materials and utilizing the PRLM RACE kit (Applied Biosystems), we generated 5′ and 3′ end libraries and performed PCR followed by sequencing to identify the mouse *Bdnf*-AS transcript. We excised the 3′ and 5′ PCR products of both mouse and human from an agarose gel and cloned them into the T-Easy vector (Promega). We sequenced positive colonies from each series.

rtPCR. We carried out rtPCR with the GeneAmp 7900 machine (Applied Biosystems). cDNA synthesis reaction contained random hexamers, 200–400 ng of RNA, 2.5 mM mixture of dNTP, $MgCl_2$ and appropriate buffer. The PCR reactions contained 20–40 ng cDNA, Universal Mastermix, 300 nM of forward and reverse primers, and 200 nM of probe in a final reaction volume of 15 µl. We designed the primer/probe set using FileBuilder software (Applied Biosystems). Primers were strand specific for sense-antisense pairs and the probes covered exon boundaries to eliminate the chance of genomic DNA amplification. The PCR conditions for all genes were as follows: 50 °C for 2 min then 95 °C for 10 min then 40 cycles of 95 °C for 15 s and 60 °C for 1 min (50 cycles for mouse *Bdnf*-AS). The results are based on cycle threshold (Ct) values. We calculated the differences between the Ct values for experimental and reference genes (18S RNA) as ΔΔCt and graphed them as a percent of each RNA to the calibrator sample. We assessed the relative expression of *BDNF* and *BDNF*-AS RNA transcripts in several human and mouse cell lines by rtPCR. We measured the expression of *Bdnf* and *Bdnf*-AS transcripts in several mouse brain regions and other mouse tissues, including: testis, ovary, liver, spleen, thymus, lung, kidney, heart, embryo and cerebellum in wild-type C57BL/6 mice ($n = 3$) by rtPCR.

We measured the expression of both transcripts in a commercially available panel of human tissue RNA samples (Ambion), including: total brain, cervix, ovary, spleen, kidney, testis, esophagus, thyroid, adipose, skeletal muscle, bladder, colon, small intestine, liver, lung, prostate, heart, trachea, thymus and whole embryo. We measured expression of both transcripts in a panel of commercially available, 12-week-old embryonic RNA samples (Ambion), including: embryonic brain, liver, lung, heart, kidney, muscle and whole embryo.

We measured expression of *Bdnf* and *Bdnf*-AS in a panel of monkey brain RNA samples ($n = 2$) by rtPCR using human primers and probe. The brain regions tested from the monkey samples were: (i) motor cortex, (ii) frontal cortex, (iii) hippocampus, (iv) amygdala, (v) motor cortex, (vi) insula, (vii) temporal cortex, (viii) interior partial cortex, (ix) striatum, (x) cerebellum, (xi) striatum, (xii) septum, (xiii) occipital cortex and (xiv) pituitary gland. Both *BDNF* and *BDNF*-AS transcripts were expressed in many tissues and cell lines tested, and the expression of *BDNF* mRNA was 10- to 100-fold greater than the *BDNF*-AS transcript.

RNA extraction and rtPCR of the mouse brain samples. We euthanized mice after 28 d and excised the brains. One hemibrain from each mouse was fixed in 4% formaldehyde overnight for histological studies. We excised another hemibrain for RNA quantitative measurement from the hippocampus, frontal cortex and hypothalamus. We extracted RNA after homogenization in Trizol reagent (Invitrogen) according to the manufacturer's protocol. We separated the aqueous phase and added an equal volume of 70% ethanol before passing the samples through Qiagen RNeasy columns (QIAGEN) and we subjected those RNA samples to on-column DNAse treatment for removal of DNA contamination. We used 400 ng of each sample for the first-strand cDNA synthesis and carried out rtPCR measurements as described above. We plotted the percentile changes in RNA levels, for individual tissues as compared to control mice, in each graph.

Cell culture and transfection. We purchased human cortical neurons, HCN-1A, originating from the brain of an 18-month-old female (ATCC). These cells were reported to be positive for a number of neuronal markers including neurofilament protein, neuron specific enolase and gamma aminobutyric acid. We cultured cells in a DMEM medium supplemented with 10% FBS. We purchased human glial cells (ATCC) that originated from the brain of a 33-year-old male with malignant glioblastoma. We cultured these cells in a mixture of DMEM and F12 plus 10% FBS, 1% NEAA, 2.5 mM L-glutamate, 15 mM HEPES, 0.5 mM sodium pyruvate and 1% sodium bicarbonate. We cultured HEK293T, N2a, human cortical neuron (HCN1) and human glioblastoma MK059 cells in appropriate medium, and transfected cells in logarithmic growth, with 5–20 nM of siRNA or antisense oligonucleotides using 0.2% lipofectamine 2000 (Invitrogen), according to manufacturer's instructions. Antisense oligonucleotides are single-stranded, 14-nucleotide DNA strands with 2′-*O*-methyl and LNA modifications, complementary to the *BDNF*-AS sequence. We designed 14 functional and two inert control oligonucleotides (that do not have targets in the mammalian genome). Cells were incubated for various time points before RNA extraction, using Qiagen RNeasy columns.

Stability and α-amanitin treatment. We plated HEK293T cells into 6-well plates. We treated cells 24 h later with 50 mg/ml of α-amanitin and harvested cells for RNA purification and rtPCR at 6, 12 and 24 h after treatment. We collected three independent samples for each data point and all experiments included untreated matching samples for RNA purification and data analysis.

Statistical analysis. We did all experiments with 6–20 biological and 3–6 technical repeats. The data presented in the graphs are a comparison with control-treated groups after post-hoc analysis of the corresponding treatment factor using main effects in a two-way analysis of variance (ANOVA). We calculated the significance of each treatment as a *P*-value. As depicted in each graph, ($P < 0.05$) was considered significant.

Western blot analysis. We transfected HEK293T cells with 10 nM of *BDNF*-AS, or control siRNA. We disrupted cells, 48 h after transfection, with 200 µl of Laemmli sample buffer (Bio-Rad) containing 350 mM DTT. We separated 20 µl of the lysate on a 10% SDS PAGE and transferred it to a nitrocellulose membrane overnight. Then we incubated the membrane with primary antibody for MecP2 (Abcam), *BDNF* (Promega) and secondary antibody conjugated to horseradish peroxidase. After addition of HRP substrate, we detected the

doi:10.1038/nbt.2158

chemiluminescent signal with X-ray film. We stripped the same membrane and reused it for detection of β-actin as a loading control.

ELISA. We transfected cells with 20 nM of *BDNF*-AS siRNA or control siRNA. The cell supernatant was collected for ELISA experiments. Alternatively, we extracted total protein from mouse brain tissues embedded in protein extraction buffer plus protease inhibitors (BCA kit, Fisher) and homogenized with the bioruptor and metal beads. Total protein was measured using BCA protein assay kit (Pierce) and sample loads were normalized to total protein concentrations. We purchased the ELISA kits for human BDNF from Promega (catalog number G7611) or mouse Bdnf from Millipore (catalog number CYT306) and we performed ELISA following the supplier's protocol. We subtracted average absorbance of three repeats at 450 nm from background and normalized it to the control sample.

Dissecting mouse hippocampal neural stem cells in neurospheres. We separated neuronal stem cells from the hippocampus of mouse pups, P0-P1. The hippocampi were mechanically separated to single cells, collected by short spins and grown in a mixture of DMEM and F12, containing glutamine, antibiotics, B27 solution and 0.001 mM concentration of both EGF and FGF. After 3–4 d floating neurospheres formed (neurosphere cell processing and immunocytochemistry techniques have previously been published[50]). We plated 100,000 cells in 24-well plates coated with poly-L-lysine (PLL). The plating of neurosphere cells onto PLL starts the differentiation process. On the third day after plating, we removed growth factors from the medium and allowed the cells to grow for 4 more days (7 d post-plating). By this time, the cell culture had a mix of neural cell lineages consisting of astrocytes, neurons, oligodendrocytes and their progenitors, making it more similar to mature brain tissue. We measured the expression of *Bdnf* and *Bdnf*-AS in floating neurospheres as well as in 3 and 7 d post-plating cultures. We performed knockdown experiments, using either 50 nM siRNAs or 20 nM antisense oligonucleotides targeting *Bdnf*-AS transcript, at 3 or 7 d post-plating.

Neural stem cells are also seeded in immunocytochemistry chambers, (18,000 cell per well) in a total volume of 80 µl. We next transfected neurospheres, using the same protocol, to assess the functional effects of *Bdnf*-AS knockdown on murine primary cells. After 48–72 h, cells were fixed with paraformaldehyde (4%) for 20 min and washed with 1× PBS several times. After blocking with FBS, neurospheres were incubated with primary antibody (monoclonal rabbit β-tubulin III, TUJ1) at a 1:2,000 concentration overnight. Fixed cells were incubated with secondary antibody, labeled with Alexafluor 568 (goat anti-rabbit IgG, 2 mg/ml, at concentration of 1:5,000). Nuclei were stained with Hoechst stain[50]. Images were obtained by immunofluorescence antigen detection microscopy.

50. Lopez-Toledano, M.A. & Shelanski, M.L. Neurogenic effect of beta-amyloid peptide in the development of neural stem cells. *J. Neurosci.* **24**, 5439–5444 (2004).